


FRONTIER LETTER

Open Access



Structural heterogeneity in and around the fold-and-thrust belt of the Hidaka Collision zone, Hokkaido, Japan and its relationship to the aftershock activity of the 2018 Hokkaido Eastern Iburi Earthquake

Takaya Iwasaki^{1*} , Noriko Tsumura², Tanio Ito³, Kazunori Arita⁴, Matsubara Makoto⁵, Hiroshi Sato¹, Eiji Kurashimo¹, Naoshi Hirata¹, Susumu Abe⁶, Katsuya Noda⁷, Akira Fujiwara⁸, Shinsuke Kikuchi⁹ and Kazuko Suzuki¹⁰

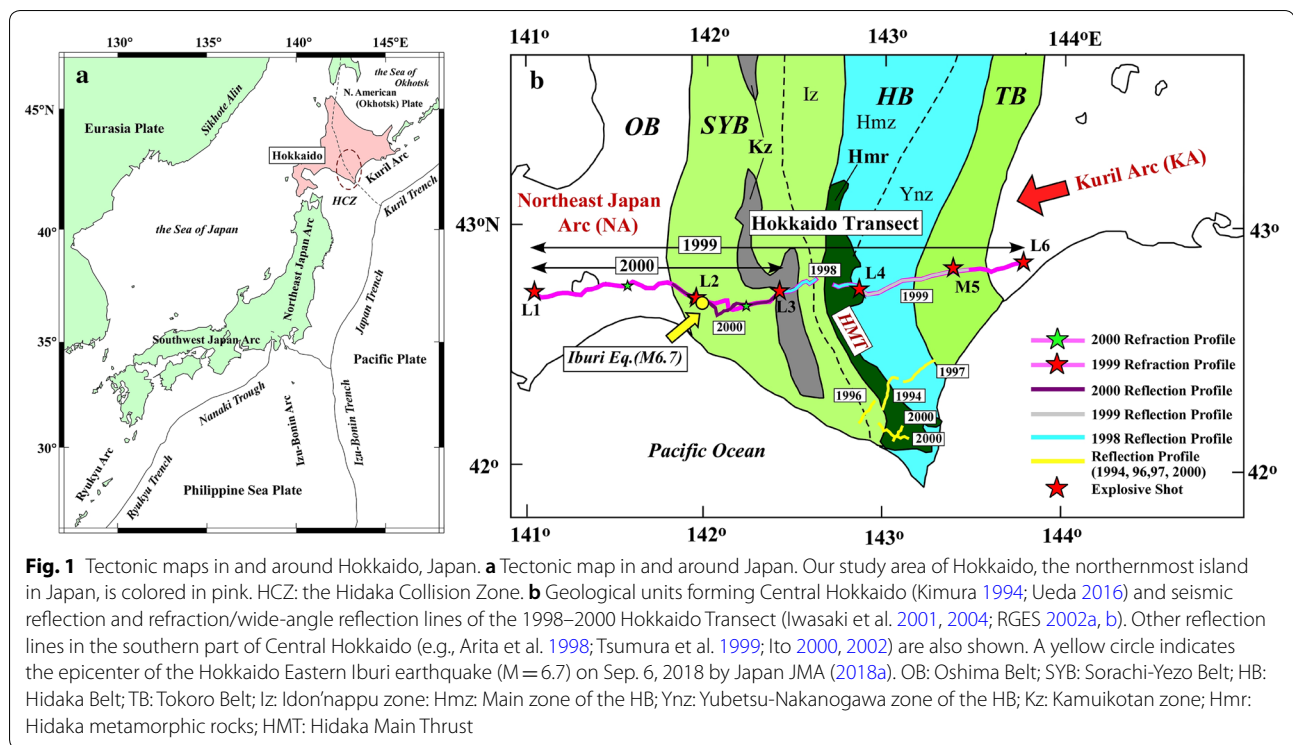
Abstract

The Hokkaido Eastern Iburi Earthquake ($M = 6.7$) occurred on Sep. 6, 2018 in the southern part of Central Hokkaido, Japan. Since Paleogene, this region has experienced the dextral oblique transpression between the Eurasia and North American (Okhotsk) Plates and the subsequent collision between the Northeast Japan Arc and the Kuril Arc due to the oblique subduction of the Pacific Plate. This earthquake occurred beneath the foreland fold-and-thrust belt of the Hidaka Collision zone developed by the collision process, and is characterized by its deep focal depth (~ 37 km) and complicated rupture process. The reanalyses of controlled source seismic data collected in the 1998–2000 Hokkaido Transect Project revealed the detailed structure beneath the fold-and-thrust belt, and its relationship with the aftershock activity of this earthquake. Our reflection processing using the CRS/MDRS stacking method imaged for the first time the lower crust and uppermost mantle structures of the Northeast Japan Arc underthrust beneath a thick (~ 5 – 10 km) sedimentary package of the fold-and-thrust belt. Based on the analysis of the refraction/wide-angle reflection data, the total thickness of this Northeast Japan Arc crust is only 16–22 km. The Moho is at depths of 26–28 km in the source region of the Hokkaido Eastern Iburi Earthquake. Our hypocenter determination using a 3D structure model shows that most of the aftershocks are distributed in a depth range of 7–45 km with steep geometry facing to the east. The seismic activity is quite low within the thick sediments of the fold–thrust belt, from which we find no indication on the relationship of this event with the shallow (< 10 – 15 km) and rather flat active faults developed in the fold-and-thrust belt. On the other hand, a number of aftershocks are distributed below the Moho. This high activity may be caused by the cold crust delaminated from the Kuril Arc side by the arc–arc collision, which prevents the thermal circulation and cools the forearc uppermost mantle to generate an environment more favorable for brittle fracture.

Keywords: The Hokkaido Eastern Iburi Earthquake, Hokkaido, Arc–arc collision, Fold-and-thrust belt, Seismic structure, Controlled source seismic experiments

*Correspondence: iwasaki@eri.u-tokyo.ac.jp

¹ Earthquake Research Institute, the University of Tokyo, Tokyo, Japan
Full list of author information is available at the end of the article



Introduction

The Hokkaido Eastern Iburi Earthquake ($M=6.7$), hereafter called as the Iburi Earthquake, took place on Sep. 6, 2018 in the southern part of Central Hokkaido (The Headquarters for Earthquake Research Promotion (HERP) 2018a, b, c; Fig. 1). The source region of this earthquake is located beneath the foreland fold-and-thrust belt of the Hidaka Collision zone which has been formed by the collision between the Kuril Arc and the Northeast Japan Arc (NE Japan Arc) since Middle Miocene. The Iburi Earthquake has interesting characteristics. First, it occurred at a very deep depth (~ 37 km) (Japan Meteorological Agency (JMA) 2018a). Aftershocks of this event by JMA (2018a) are also distributed in a deeper depth range of 12–45 km. These observations generated intense debates on whether this event occurred in the crust or the uppermost mantle. Second, the CMT solution shows a reverse fault with ENE–WSW P axis (JMA 2018b), while the focal mechanism from first motion data indicates a dextral strike-slip fault (JMA 2018c; National Research Institute for Earth Science and Disaster Resilience (NIED) 2018). Based on SAR and GNSS data, Geospatial Information Authority of Japan (GSI) (2018) presented a preliminary model for this earthquake which is characterized as a reverse fault steeply inclining to the east with 14-km length, 16-km width and 1.3-m slip. These indicate the complicated rupture process of this event, namely, the beginning of

the rupture was of a strike-slip type, which was followed by the main rupture of a reverse fault type. Such features of this earthquake were probably controlled by significant structural heterogeneity in and around the source region.

The “Hokkaido Transect” was an intensive seismic project with controlled sources undertaken in 1998–2000 (Iwasaki et al. 2001, 2004; the Research Group for Explosion Seismology, Japan (RGES) 2002a, b; Fig. 1b). The profile lines of this project were laid out from the hinterland to the foreland fold-and-thrust belt crossing the Hidaka Main Thrust (see “Geological setting in and around the source region of the Hokkaido Eastern Iburi Earthquake” section) in Central Hokkaido, involving the source region of the Iburi Earthquake. The seismic refraction/wide-angle reflection data from the Hokkaido Transect clarified crustal deformation due to the above arc–arc collision and complicated structural variation in the fold-and-thrust belt (Iwasaki et al. 2004). But, as described in “Reprocessing and reanalyses for controlled source seismic data” section, deeper structures including the lower crust and the uppermost mantle, which are inevitably important to understand the mechanism on the occurrence of the deep Iburi Earthquake, remain enigmatic. In this paper, we reanalyze the data from the Hokkaido Transect by advanced processing and interpretation techniques, especially focusing on the unknown deeper structures. Then, aftershock distribution of the Iburi Earthquake is intensively investigated based on

the newly obtained structural constraints down to the upper mantle. Finally, we discuss the occurrence of this event under a wider tectonic scope in and around Central Hokkaido.

Geological setting in and around the source region of the Hokkaido Eastern Iburi Earthquake

The seismic profiles of the Hokkaido Transect are crossing main geological units covered with in-and-after Middle Miocene strata in Central Hokkaido (Fig. 1b). The Oshima Belt (OB), which is northern extension of the NE Japan, has been formed by westward subduction and accretion processes at the eastern margin of the Asian Continent (e.g., Kiminami and Kotani 1983; Niida and Kito 1986). The Sorachi-Yezo Belt (SYB) is comprised of a Jurassic ophiolite and Cretaceous accretionary complexes (Sorachi Group) which are overlain by Cretaceous forearc basin clastic rocks (Yezo Group). The Iton'napu zone (Iz) consists of Cretaceous accretionary complexes (Kiyokawa 1992; Ueda et al. 2001). The Kamuikotan zone (Kz) is characterized by High P-Low T metamorphic rocks originated from the underlying Cretaceous accretionary complexes, and associated ultramafic rocks (Ueda 2005). The Hidaka Belt (HB) is divided into the Main zone (Hmz) and Yubetsu-Nakanogawa zone (Ynz) (Ueda 2016). The Hmz is a Paleogene accretionary complex. The units from the SYB to Hmz were also formed by the westward subduction. On the other hand, the Ynz and the Tokoro Belt (TB) are accretionary complexes of northward or eastward subduction along the paleo-Kuril arc-trench system in Paleogene and Cretaceous, respectively (Kiminami and Kotani 1983; Niida and Kito 1986; Nanayama et al. 1993; Ueda 2016).

Since Paleogene, Central Hokkaido has been highly deformed under the dextral oblique collision between the Eurasia and North American (Okhotsk) Plates and the following westward movement of the Kuril Arc due to the oblique subduction of the Pacific Plate. The latter event, which started in Middle Miocene, has formed the Hidaka Collision zone (HCZ) with the uplift of High T-Low P Hidaka metamorphic rocks (Hmr) along the Hidaka Main Thrust (HMT) (Komatsu et al. 1983; Kimura et al. 1983; Kimura 1986). A series of reflection surveys in 1994, 1997 and 1998 in the southern part of the HCZ (Fig. 1b) revealed clear crustal delamination. Namely, the upper 23-km crust in the Kuril Arc side, which corresponds to the Hmr, is thrust up along the HMT; while, the lower part of the crust descends down to the west (Arita et al. 1998; Tsumura et al. 1999; Ito 2000, 2002). Refraction/wide-angle reflection experiments in the Hokkaido Transect showed the similar crustal obduction occurring in the northern part of the HCZ (Iwasaki et al. 2004).

The collision of the Kuril arc is also responsible for the development of the fold-and-thrust belt west of the HMT. In this belt, the west-verging structure has been growing especially within the thick (~10 km) Cenozoic sedimentary package (PN and M in Fig. 2a), whose western margin is known as the active fault zone (East Boundary Fault zone of the Ishikari Lowland, see “[After-shock distribution of the 2018 Hokkaido Eastern Iburi Earthquake](#)” section). Previous seismic expeditions support the above structural features. The seismic data of the Hokkaido Transect showed a very thick (~5–10 km) sedimentary package with velocity reversals on the top of the SYB (Iwasaki et al. 2004). According to the reprocessing for the previous seismic reflection surveys, active faults in the thick sedimentary package generally dip eastward, getting very gentle at depth levels shallower than 10–15 km (Ito 2000; Kazuka et al. 2002).

The Iburi Earthquake took place beneath the fold-and-thrust belt at a deep depth of ~37 km. Seismic activity west of the HMT is also characterized by very deep (more than 20–30 km) earthquakes including M7 class events (Moriya 1972; Iwasaki et al. 1983; Moriya et al. 1983; Kita et al. 2012). The seismological structure around the source regions of these events is highly complicated (Takanami 1982; Miyamachi and Moriya 1984; Miyamachi et al. 1994; Iwasaki et al. 1998, 2004; Moriya et al. 1998; Murai et al. 2003; Kita et al. 2012). However, the relationship between such structural heterogeneity and characteristics of seismic activity is left unclarified as yet.

Reprocessing and reanalyses for controlled source seismic data

In the 1998–2000 Hokkaido Transect, a series of seismic experiments with controlled sources were undertaken in the northern part of the HCZ (Fig. 1, Tables 1 and 2). The 1998 reflection survey was aimed to elucidate the collision structure around the HMT by 15- and 10-km profiles (Iwasaki et al. 2001). A 227-km refraction/wide-angle reflection line in 1999 was laid out from the hinterland to the fold-and-thrust belt crossing the HMT to obtain the whole velocity structure of the HCZ (RGES 2002a). At the same time, seismic reflection data were acquired along a 58-km line in the hinterland area east of the HMT. The 2000 seismic survey, on the other hand, was focused on investigating the structure of the fold-and-thrust belt west of the HMT both from reflection and refraction/wide-angle reflection experiments with profile lengths of 70 and 114 km, respectively (RGES 2002b). Iwasaki et al. (2004) presented a velocity structure model from the 1999 and 2000 refraction/wide-angle reflection data. For the 1998 and 1999 reflection data, Adachi (2002) imaged the collision structure along

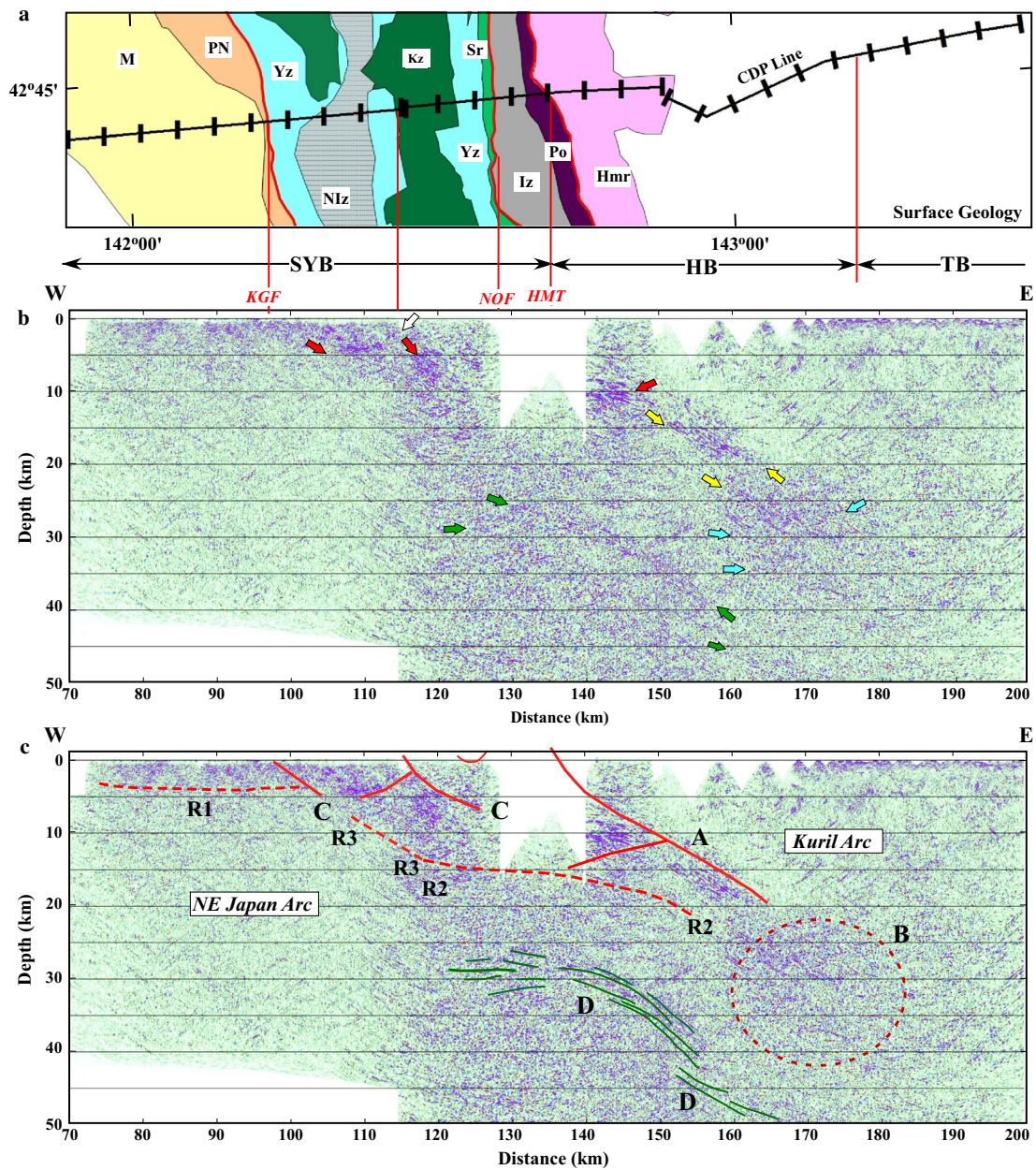


Fig. 2 Surface geology and depth-migrated section. **a** Surface geology. Hmr: Hidaka metamorphic rocks; Po: Poroshiri Ophiolite; Iz: Idon’napu zone; Sr: Sorachi Group; Yz: Yezo Group; Kz: Kamuikotan zone; NIz: Nappe of Iz; PN: Poronai Group; M: Miocene strata; HMT: Hidaka Main Thrust; NOF: Nitarachi-Oshorobetsu fault; KGF: Kenomai-Gabari fault. **b** Depth-migrated section from 1998–2000 seismic reflection data using CRS/MDRS method (see the text for detailed explanation). Yellow arrows show eastward dipping events beneath the HB. This domain is traced down to a 20–25-km depth. At depths of 25–40 km beneath the HMT, several uncoherent events are recognized (light blue arrows). West-verging events in the uppermost 15-km crust west of the HMT are also noticed (red arrows). A white arrow is the uppermost event dipping to the west. **c** Depth-migrated section from 1998–2000 seismic reflection data with our interpretations (red lines). “A” indicates the deeper image of the HMT. Uncoherent events around the bottom of the HMT are enclosed by a broken ellipse (“B”). West-verging events in the uppermost crust are indicated by “C”. Deep structures in the NE Japan Arc are shown by green lines (“D”). Red broken lines (“R1” to “R3”) are structural boundaries interpreted with aid of the velocity structure model from the refraction/wide-angle reflection data (see Fig. 5b)

Table 1 Seismic reflection experiments in the Hokkaido Transect Project

Profile	1998-W ^a	1998-E ^a	1999 ^b	2000 ^c
Source	Vibrator x 4 + explosive	Vibrator x 4 + explosive	Explosive	Vibrator x 4 + explosive
Shot interval (m)	200–300	200–300	~1000	200–300
Charge size of explosive (kg)	100	100	40–700	100–300
Number of shots	50 + 1	24 + 1	28	161 + 4
Receiver interval (m)	50/150	50	50	50/300
Number of receivers	312	200	1055	1073
Profile length (km)	15	10	58	70
Sampling interval (ms)	4	4	4/10	4/10
Record length(s)	20/40	20/40	30	16/20/60

^a Iwasaki et al. (2001)^b RGES (2002a)^c RGES (2002b)**Table 2 Seismic refraction/wide-angle reflection experiments in the Hokkaido Transect Project**

Profile	1999 ^a	2000 ^b
Source	Explosive	Explosive
Number of shots	6	4
Charge size (kg)	100–700	100–300
Number of receivers	297	327
Profile length (km)	227	114
Sampling interval (ms)	10	10
Record length(s)	60	60

^a RGES (2002a)^b RGES (2002b)

the HMT. Although these studies revealed the complex structural variation in the HCZ to some extent, the deeper structures, particularly those of the NE Japan Arc crust and upper mantle beneath the fold-and-thrust belt, are left unclarified. In this paper, we performed intensive and integrated interpretations both for the seismic reflection and refraction/wide-angle reflection data described above.

Seismic reflection processing

To obtain deeper and broader seismic image in the HCZ, we applied recently developed and advanced processing of Common Reflection Surface (CRS)/Multi-Dip Reflection Surface (MDRS) stacking method to the combined data set of the 1998, 1999 and 2000 experiments. In the conventional Common Mid-Point (CMP) method, traces with the same mid-point are collected for stacking. In the CRS method (Hubral et al. 1999; Jäger et al. 2001; Berkovitch et al. 2008); on the other hand, traces sharing the same reflection surface are stacked and processed. This

can dramatically increase in number of stacked traces, which enables us to get clearer and more reliable seismic images as compared with the CMP method. The MDRS method is also a useful technique for imaging reflectors closely distributed with different dips, which are sometimes failed to be differentiated in the conventional processing (Aoki et al. 2010).

In Fig. 2, the depth-migrated reflection image obtained is shown together with the surface geology, our event identifications and interpretations. The CDP line for our processing is also given in the geological map (Fig. 2a). Arrows in Fig. 2b show major events we recognized. We notice a 5-km-thick and densely reflective domain composed of eastward dipping events beneath the HB (yellow arrows in Fig. 2b). This domain is traced down to a 20–25-km depth in a distance range of 155–165 km. We interpreted its easternmost/uppermost margin to be the deeper image of the HMT (“A” in Fig. 2c). At depths of 25–40 km beneath the HMT, several uncoherent events are recognized (light blue arrows in Fig. 2b), which are probably related to the deep crustal deformation in the Kuril Arc side (a broken ellipsis “B” in Fig. 2c). West-verging events in the uppermost 15-km crust west of the HMT (red arrows in Fig. 2b) are interpreted to be the faults and structural boundaries formed by the collision process (“C”; see also Fig. 2a). As stated in detail in “Straight forward modelling by ray-tracing” section, some parts of the reflection image are well correlated with layer boundaries deduced from the refraction/wide-angle reflection analyses by Iwasaki et al. (2004) and present study (see “Refraction/wide-angle reflection analysis” section and Fig. 5). The Kenomai-Gabari Fault (KGF) is imaged as a bottom of the reflective band inclining to the east (Fig. 2c).

The most striking feature from the present reflection processing is a series of deep reflectors (green arrows in Fig. 2b). These reflectors are at about 30-km depth in a distance range of 125–140 km, but are continuously traced further east down to 40–45-km depths beneath the HB. We interpreted these events to be the lowermost crustal reflector (reflective lower crust) or the Moho of the NE Japan Arc descending to the east as indicated by green lines (“D”) in Fig. 2c. Then, the total thickness of the NE Japan Arc crust is about 15–23 km in a region from the eastern part of the SYB to the HB. Such a deep structure was not imaged from the conventional processing by Adachi (2002), and is the new finding by the advanced CRS/MDRS method. We used these results as constraints for modelling deeper structure in the next section.

Refraction/wide-angle reflection analysis

The present refraction/wide-angle reflection analysis was done through two steps. The previous upper and middle crustal model (Iwasaki et al. 2004) was obtained from the forward modelling of a ray-tracing method (e.g., Cervený 1985). In the first step, we checked the validity of this model using a different travel time analysis of seismic tomography. As described in “[Seismic tomography](#)” section, this step successfully showed its validity and reliability. Next, incorporating the results from the seismic reflection data in “[Seismic reflection processing](#)” section, the forward modelling by the ray-tracing method was undertaken to reveal still unknown structures of the lower crust and uppermost mantle west of the HMT using travel times observed at far offsets (80–180 km). By this analysis, we tried to find out a plausible deeper structure model including the Moho and the uppermost mantle west of the HMT with aid of the structural constraints derived from the seismic reflection processing in “[Seismic reflection processing](#)” section (Fig. 2c).

Seismic tomography

We performed the tomography analysis (Zelt and Barton 1998) to 44,616 first arrival times from 88 shots both on the seismic reflection and refraction/wide-angle reflection lines. These travel times were picked within offsets of 80–150 km. According to the previous analysis, the rays of these first arrivals penetrated in the upper/middle crust shallower than ~20-km depth (see Figs. 5, 8 and 9 in Iwasaki et al. (2004)). Namely, this tomography analysis was expected to provide an “objective” model shallower than this depth.

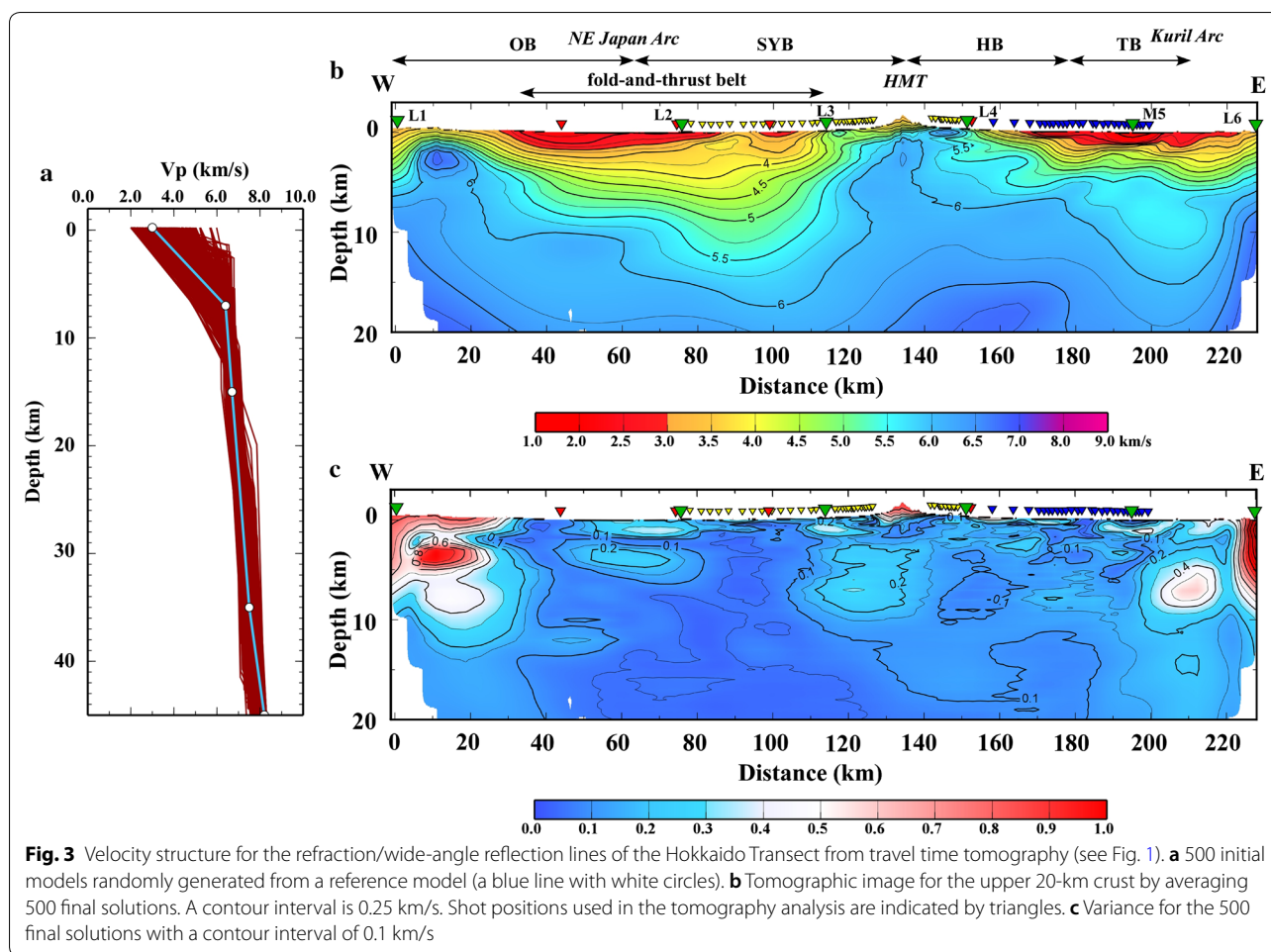
In this analysis, the stochastic approach was applied to suppress the initial model dependency in the final solution. Namely, the same travel time data were inverted 500 times for different initial models randomly generated

from a reference model (Fig. 3a). Figure 3b, c shows the average and variance of the 500 final solutions, respectively. The travel time residual of this average model is 138 ms, which corresponds to about 75% reduction from the cases of the initial models (~600 ms). The variance of the solutions is 0.1–0.2 km/s in a distance range of 20–220 km, although it exceeds 0.4–0.8 km/s near the edges of the profile (Fig. 3c). The results of checker board test are shown in Fig. 4. For 5%-velocity anomaly with a size of 20 km (horizontal direction) × 5 km (depth direction), our data have enough resolving power down to ~10–12 km in almost the entire part of the profile (Fig. 4a). For a smaller anomaly (10 km × 3 km), the resolution becomes worse in a distance range of 0–70 km due to the sparse shot spacing, but the anomaly pattern is recovered down to 8–10-km depth (Fig. 4b).

The obtained model (Fig. 3b) is characterized by a very thick (~10–12 km) low velocity (2–5.5 km/s) body in the fold-and-thrust belt, the outcrop of higher velocity (>5.8–6 km/s) material around the HMT, and again a thick (~5–6 km) low velocity body in the hinterland east of the HMT. The equi-velocity lines of 5.5 and 6.0 km/s in the western part of the profile are descending to the east from 7–10 km under the westernmost edge of the profile to 15–18-km depth beneath the eastern part of the fold-and-thrust belt, representing the underthrust of the upper crust of the NE Japan Arc from the west. All of these features are well consistent with the previous upper/middle crust model presented by Iwasaki et al. (2004), strongly confirming the validity and reliability of their model (see also Fig. 5a).

Straight forward modelling by ray-tracing

Based on the result in “[Seismic tomography](#)” section, we adopted the velocity model by Iwasaki et al. (2004) as an upper/middle crustal part of our model (Fig. 5a). Before proceeding to the modelling for the deeper structure, we directly compared this velocity model with the seismic reflection image (Fig. 5b). As stated in “[Seismic reflection processing](#)” section, some of the layer boundaries in the upper/middle crust are well correlated with the reflection image (see “R1” to “R3” in Figs. 2c, 5a, b). A rather flat reflection boundary (“R1”) beneath the Miocene strata (M) is explained as a layer boundary existing in the thick sedimentary package (see also Fig. 5a). The top of reflectors distributed in a depth range of 15–25 km beneath the HB and the eastern SYB (“R2”) corresponds well to the upper interface of the 5.4–5.5 km/s layer, which is interpreted to be the uppermost part of the crystalline crust of the NE Japan Arc (Iwasaki et al. 2004). The reflection boundary “R3” beneath the SYB, which corresponds to the eastern margin of the 5.3–5.6 km/s body (Fig. 5a), is probably the downward continuation of the



Kenomai-Gabari Fault (KGF) (see “[Seismic reflection processing](#)” section and Fig. 2c). It is also noted that these layer boundaries of R1–R3 have a higher velocity contrast of 0.3–1.0 km/s.

In determining the deeper structure, particularly beneath the fold-and-thrust belt including the source region of the Iburu Earthquake, we used travel times of several phases recognized at far offsets (~80–180 km) provided from the 1999 refraction/wide-angle reflection experiment (Fig. 6). Although these data contain some structural information on the lower crust and upper mantle, they are not of good quality. So, most of these data were used neither in the former study by Iwasaki et al. (2004) nor in the present tomography analysis because their phase identifications are more or less ambiguous and not unique.

The present seismic reflection processing in “[Seismic reflection processing](#)” section, however, succeeded in imaging the deeper geometry of the NE Japan Arc crust west of the HMT (Fig. 2). So, if this information is incorporated in the modelling, the far-offset data mentioned

above are expected to contribute to the construction of the deeper structure. In the following analysis, we fixed the location of Moho in a distance range of 120–160 km at the bottom of the deep reflectors in the migrated depth section (“D” in Fig. 2c). Then, the configuration of Moho in a range of 0–120 and lower crustal structure (layer geometry and velocities) in a range of 0–160 km were estimated from the travel time data at far offsets. Considering the low S/N ratio of the data, we also examined the change in resultant structure model by taking alternative phase identifications to them as described below.

Figure 7 shows the record section and ray diagram for the shot L1 (Fig. 1b). On the record sections, travel time curves from the model are superimposed (Fig. 7a, b). For the first arrival, theoretical travel times (green lines) fit well to the observed ones, again indicating the validity of the upper/middle crustal structure by Iwasaki et al. (2004). In Fig. 6a, we notice weak arrivals at offsets of 80–110 km with an apparent velocity of 7.6 km/s (phase “A”). Phases “B” and “C” beyond 100-km offset are recognized as a wave train with larger amplitude. In Fig. 7a,

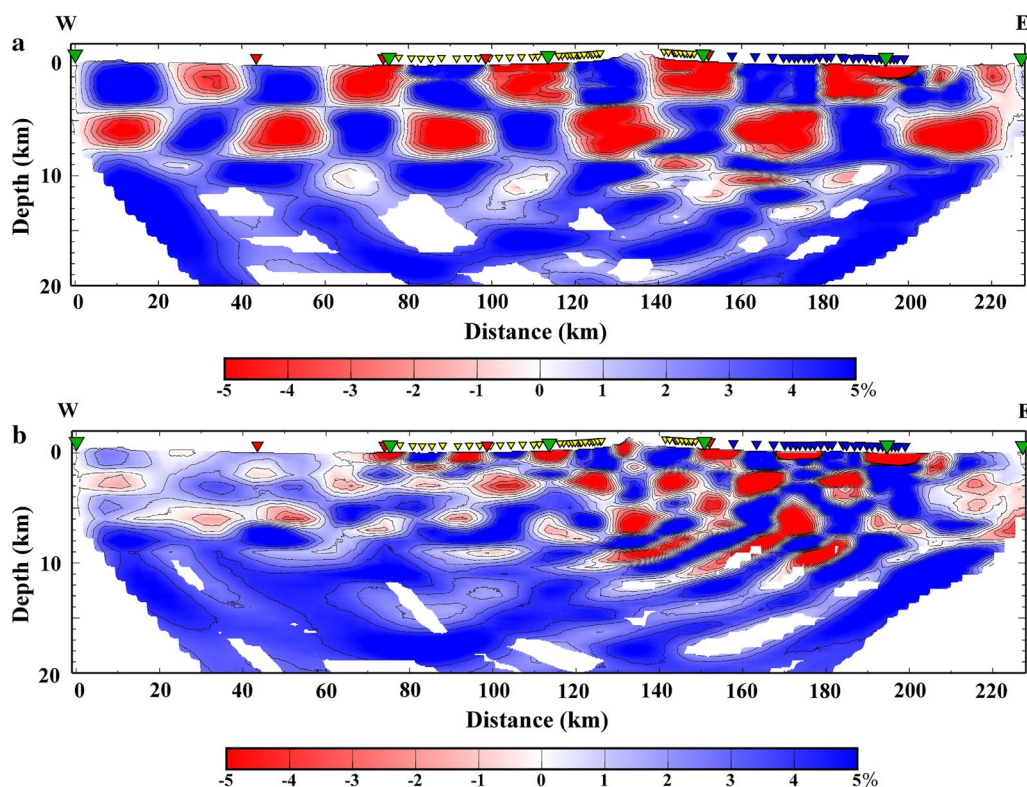


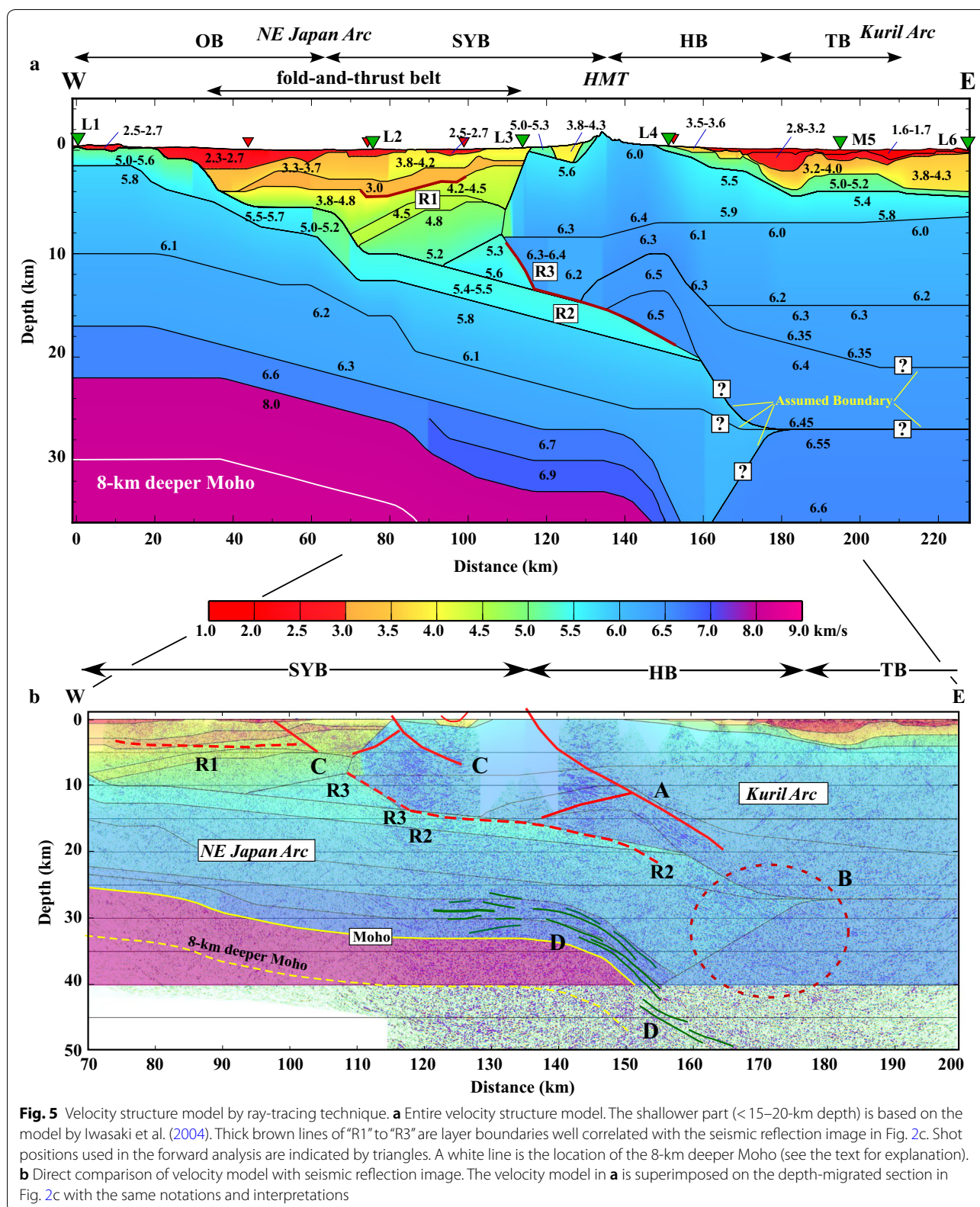
Fig. 4 Results of checker board test. **a** Case for anomaly size of 20 km (Horizontal) \times 5 km (vertical). Shot positions used in the tomography analysis are indicated by triangles. **b** Case for anomaly size of 10 km \times 3 km

the phase “A” is interpreted to be Pn wave (refracted wave from the upper mantle), while the phases “B” to “D” are explained by the superposition of reflected waves from the crust (PiP1) and Moho (PmP) (see also Fig. 7c). The travel times of the Pn and PmP phases require rather shallow Moho at a depth of about 22–33 km in the western part of the profile (a distance range of 0–120 km (Figs. 5a and 7c). The PmP phase constrained the lower crustal velocity as 6.6 km/s in a range of 0–90 km. Because the qualities of the phases “A” to “D” in Fig. 6a are not so good, an alternative phase identifications may be possible. Namely, if we neglect the very weak phase of “A” and explain the phase “C” as the Pn phase (Fig. 7b), then the Moho becomes about 8-km deeper than that in the previous case as indicated by a broken line in Fig. 7c. By this change, the onsets of PmP phase at distant offsets (>100 km) are delayed about 0.5 s, but still in the travel time range of the wave train “C” in Figs. 6a and 7c.

Figure 8 shows the case for the shot M5 (Fig. 1b). Phases “A” and “B” in Fig. 6b are interpreted to be Pn and PmP waves, respectively. These travel time data also indicate shallow Moho in a range of 0–120 km as in the case of the shot L1, but require higher velocity (~ 6.7 – 6.9 km/s) in the lower crust at around

90–160-km distances (Fig. 5a). As shown in Fig. 8b, rays of the Pn and PmP phases from this shot pass through the middle/lower crust east of the HMT (enclosed by a broken circle) in which the velocity estimation in the present analysis is still ambiguous. Relatively larger velocity changes of around 0.2–0.3 km/s in this part yield 0.2–0.3-s travel time shift for the Pn and PmP phases, but give only 2–3-km shift in Moho depth estimation. Reflections from the mid-crustal interfaces east of the HMT or those in the NE Japan Arc (for example R1 and R2 in Fig. 8b) appear in the eastern part of the profile and do not affect our interpretation for the phases “A” and “B” (Figs. 6b and 8a). If the Moho is set at 8-km deeper position (a broken line in Fig. 8b), the phase “A” at an offset range of 120–160 km (Fig. 6b) is not explained at all because the western half of the profile falls in a shadow zone for the Pn phase.

From these travel time calculations for the shots L1 and M5, we can say that the Moho depth of the NE Japan Arc is rather shallow, varying eastward from 22 to 33 km (Fig. 5a). The crustal thickness is 16–22 km. Although the observed travel times at the far offsets contain 0.3–0.5 s ambiguity, the Moho depth is constrained within an error about 8 km or less (the white line in Fig. 5a).



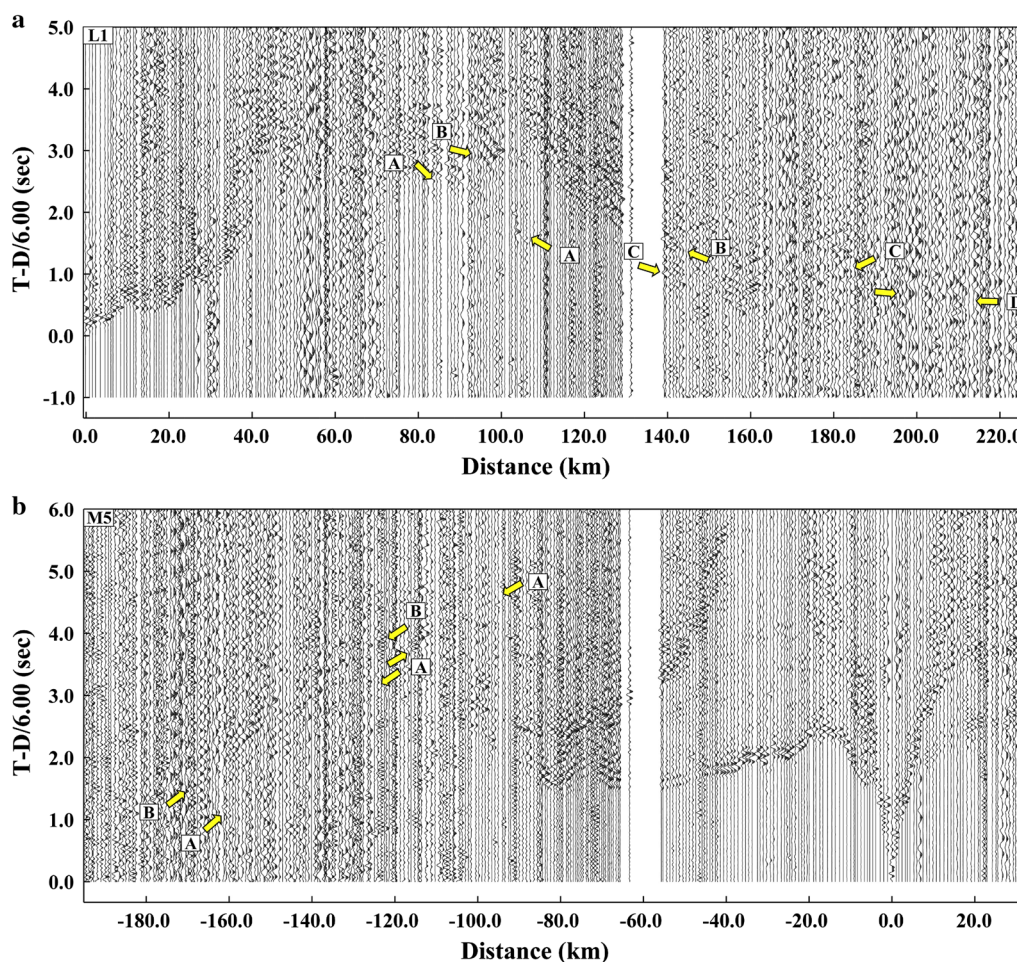


Fig. 6 Record sections from shot L1 and M5. Phases recognized at far offsets (~ 80 – 200 km) are indicated by arrows. **a** Record section from shot L1. Interpretations for the phase “A” to “D” are shown in Fig. 7a or b. **b** Record section from shot M5. Interpretations for the phase “A” and “B” are shown in Fig. 8a

Aftershock distribution of the 2018 Hokkaido Eastern Iburi Earthquake

NIED routinely determines hypocenters in and around the Japanese Islands from seismic wave data of their own seismic network (the High sensitivity seismograph network (Hi-net)) and those of JMA, universities and other institutes. A 3D structure model adopted in this hypocenter determination is based on the result of seismic tomography by Matsubara et al. (2017a). Using the same seismic networks and the structure model, we intended to relocate the main shock and aftershocks of the Iburi Earthquake. This velocity model, however, was built to express the large-scale structure in the entire part of the Japanese Islands. So, the grid size adopted in the tomographic inversion was relatively large (0.2° for horizontal direction and 5 km in depth direction). Furthermore, the distribution of seismic station is sparse in Hokkaido. From these reasons, the model by Matsubara et al.

(2017a) does not fully reflect the smaller-scale structural variation in our study area as indicated in Figs. 3 and 5a.

Before relocating and discussing the aftershock distribution, we performed test calculation using simple 1D velocity models (Fig. 9a) to examine the structure dependence of determined earthquake locations. One test model (Model 1) was constructed by simply averaging the 3D velocity model by Matsubara et al. (2017a), where the Moho is expressed as a transition zone in a depth range of 32–35 km. Another model (Model 2), which is based on our present results from “[Reprocessing and reanalyses for controlled source seismic data](#)” section (Fig. 5), has low velocity materials at its top and shallow Moho at depth of 28–30 km. This model is said to be an extreme case in examining the effect of the thick sediments to our hypocenter determination.

We selected 31 aftershocks with $M > 3.5$ for which P and S wave arrival times were carefully picked for

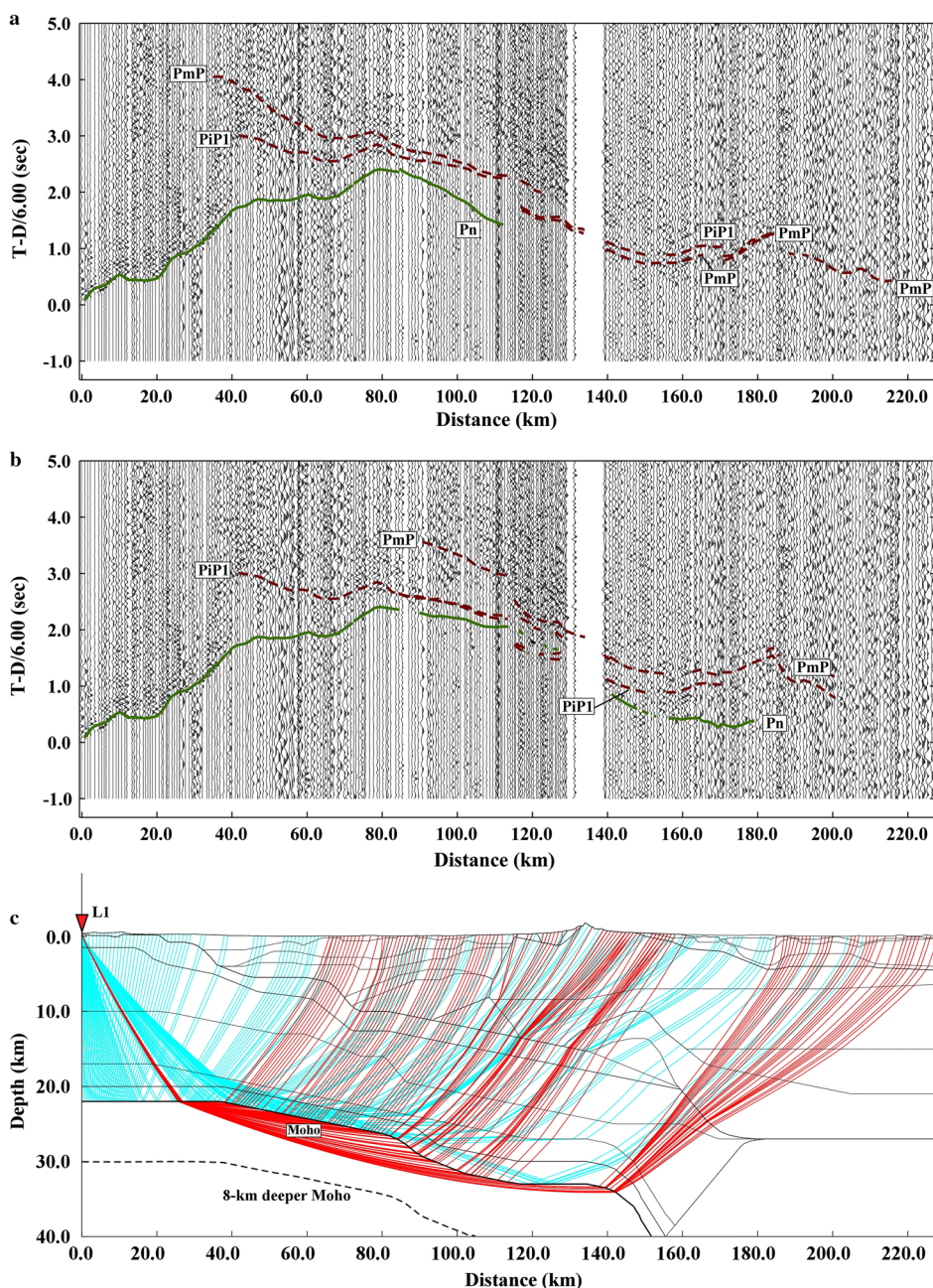
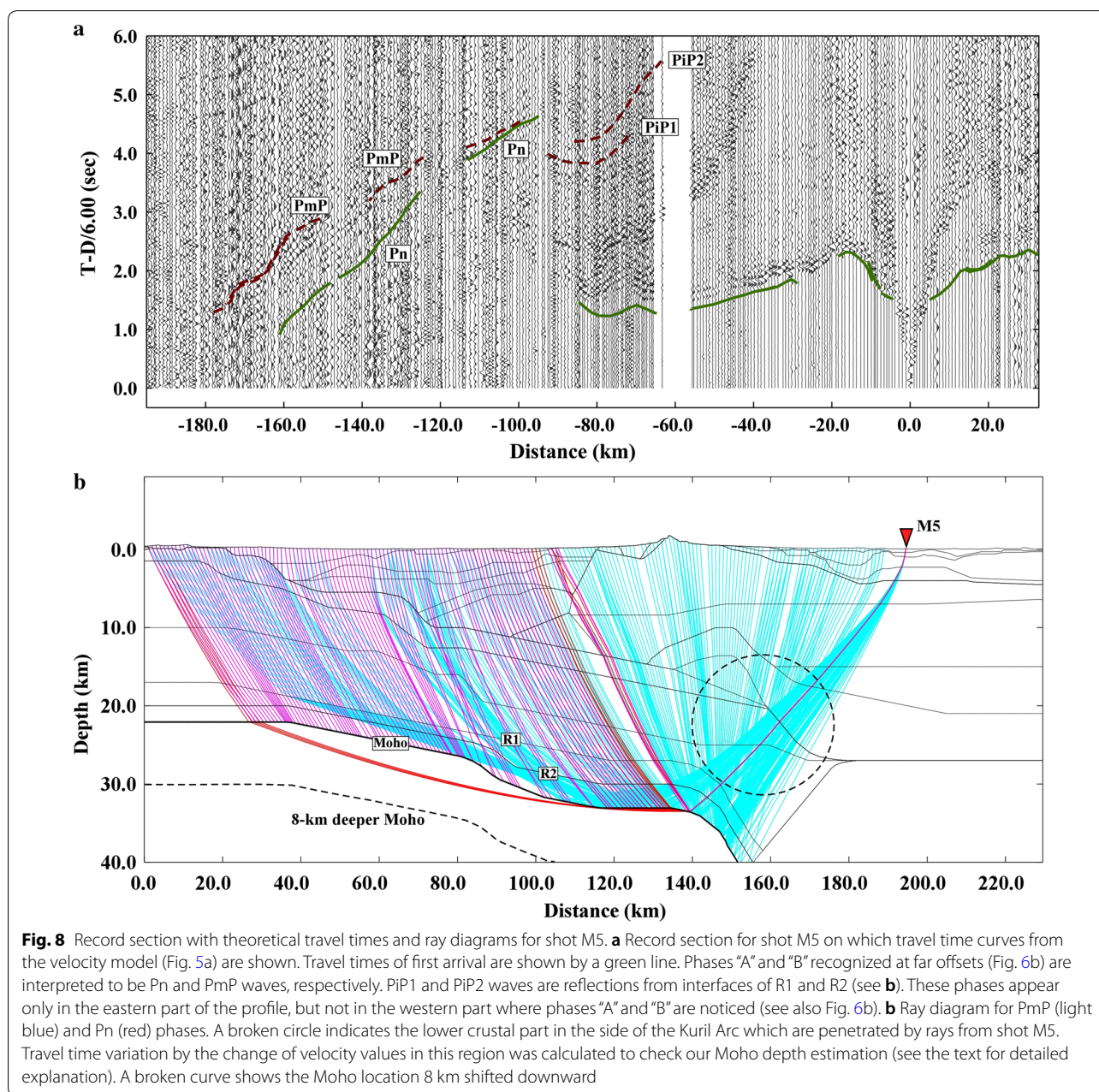


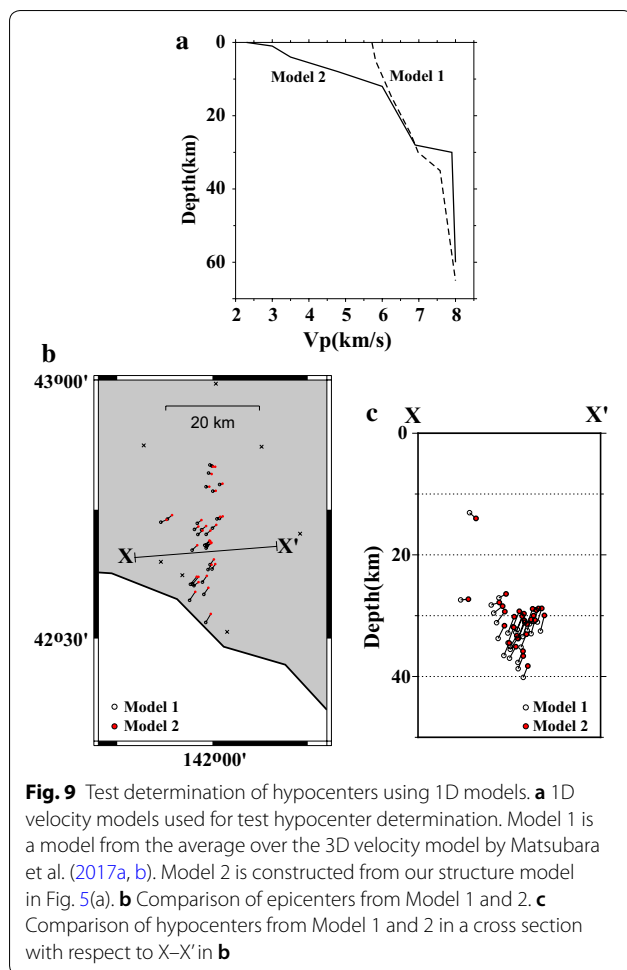
Fig. 7 Record section with theoretical travel times and ray diagrams for shot L1. **a** Record section on which travel time curves predicted from the velocity model (Fig. 5a) are shown. Theoretical travel times for first arrival and late phase are shown by a green and brown curves, respectively. See also the phase identifications in Fig. 6a. Phase “A” is interpreted to be Pn wave (refracted wave from the upper mantle), while phases “B” to “D” are explained by superposition of PiP1 and PmP waves (reflected waves from the interfaces R1 and Moho, respectively). See also ray diagrams in **c**. **b** Record section on which travel time curves from a velocity model with 8-km deeper Moho (see **c**) are shown. Theoretical travel times for first arrival and late phase are shown by a green and brown curves, respectively. See also the phase identifications in Fig. 6a. Phase “B” in Fig. 6a is interpreted to be the PiP1 phase. The onset of wave train of phase “C” is explained by Pn wave while its later part by PmP wave. **c** Ray diagrams for PmP (light blue) and Pn (red) waves. Interfaces corresponding to PiP1 wave is indicated by R1. A broken curve shows the Moho location 8 km shifted downward (see the text for detailed explanation), which corresponds to the case of **b**



seismic stations located within about 80-km distance from the aftershock area. The hypocenter determination was undertaken several times by the program code “HYPOMH” (Hirata and Matsu’ura 1987). Through these computations, station corrections and V_p/V_s values of the velocity model were estimated by trial and error, so as to remove systematic time shift of O–C residuals at the individual station. The resultant V_p/V_s is 1.73. Figure 9b, c shows the comparison of hypocenter distribution for Model 1 and Model 2, from which we notice that the difference in hypocenter

remains within ~ 1 km for epicenter and ~ 2 km for focal depth, respectively.

Figure 10 shows 3140 aftershocks occurring from Sept. 6 to Oct. 17. As in the case of the 1D model calculations, station corrections were estimated from O–C travel time residuals and applied in the hypocenter determination. Comparison of the relocated events by the 3D model with those from Model 2 also showed rather small difference (<1.5~2 km) in estimated hypocenter. Therefore, it is said from the results in Figs. 9 and 10 that the overall estimation error of hypocenter in our analysis



arising from the uncertainties of the assumed velocity model is less than 2 km after applying appropriate station corrections.

In Fig. 10, we notice the very low seismic activity within the thick sedimentary package. The Iburi Earthquake is sometimes discussed in relation to the Eastern Boundary Fault Zone of Ishikari Lowland (EBFIL) located in the western part of the fold-and-thrust belt (HERP 2018a, see Fig. 10a, b). According to the previous seismic reflection surveys, however, active faults in the sedimentary package are of a west-verging thrust type getting very gentle at a depth level shallower than 10–15 km (Ito 2000; Kazuka et al. 2002). Such fault geometry completely contradicts with the high-angle aftershock distribution (Fig. 10b).

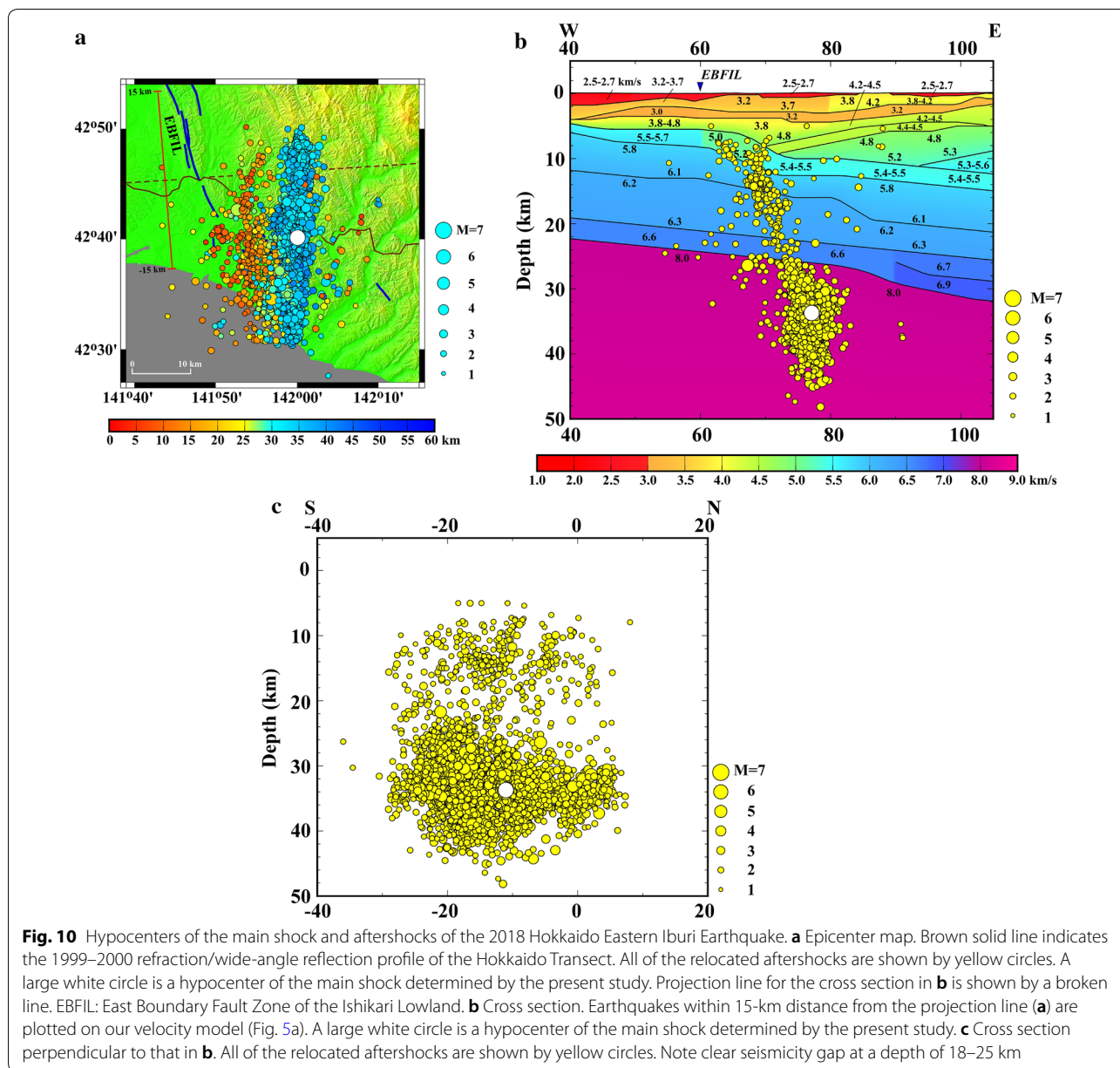
The relocated events are in a depth range of 7–45 km. Even if the estimation error of focal depth ($< \sim 2$ km) is taken into account, this range is much deeper than that of inland earthquakes in NE Japan Arc or Southwest Japan Arc (SW Japan Arc) (e.g., Omuralieva et al. 2012). The cross sections in Fig. 10b, c show that the aftershocks are separated into the upper (7–20-km depth) and lower

(22–45-km depth) groups. The seismicity gap between them is located at 20–22-km depth in the lower part of the crust in our model (Fig. 10b). This location roughly corresponds to the asperity of this earthquake determined from the joint inversion of strong motion and geodetic data (Kobayashi et al. 2019). However, the velocity model used in their analysis is different from that in our hypocenter determination, which may yield the systematic shift of the asperity location. So, the ductile property in the lower crust may not be excluded as another possibility for the gap of the aftershock activity. Furthermore, more than 80% of the relocated events are distributed in the uppermost mantle. This is the most important feature obtained from the present analysis and discussed in the next section.

Discussion

Beneath the fold-and-thrust belt (Figs. 3 and 5), the crust of the NE Japan Arc is thin (16–22 km) and the Moho deepens to the east from 22 to 33 km. The Pn velocity is estimated to be about 8 km/s. The Moho depth in this region by seismic tomography (Matsubara et al. 2017a, b), on the other hand, is about 30 km (Fig. 11). Their result, however, is probably overestimated because the travel time delay due to the low velocity sediments is not fully taken into account in their analysis (see also “[Aftershock distribution of the 2018 Hokkaido Eastern Iburi Earthquake](#)” section). Similar thin crust is also reported in the forearc basin off the NE Japan (east of the NE Japan Arc, Fig. 1a), which is considered to be structural continuation from the SYB (e.g., Finn 1994). Controlled source seismic experiments in this region indicate that the crustal thickness below the pre-Oligocene sediments is about 11–20 km and the Pn velocity is around 8 km/s (Takahashi et al. 2004; Miura et al. 2005). The tomographic studies by Nakajima et al. (2002), Yamamoto et al. (2014) and Matsubara et al. (2017a, b) also show shallower Moho at a depth of 20–30 km. These features are well consistent with our results and strongly support the thin crust in the SYB. So, we argue that the many aftershocks are occurring in the uppermost mantle of the NE Japan Arc (Fig. 10).

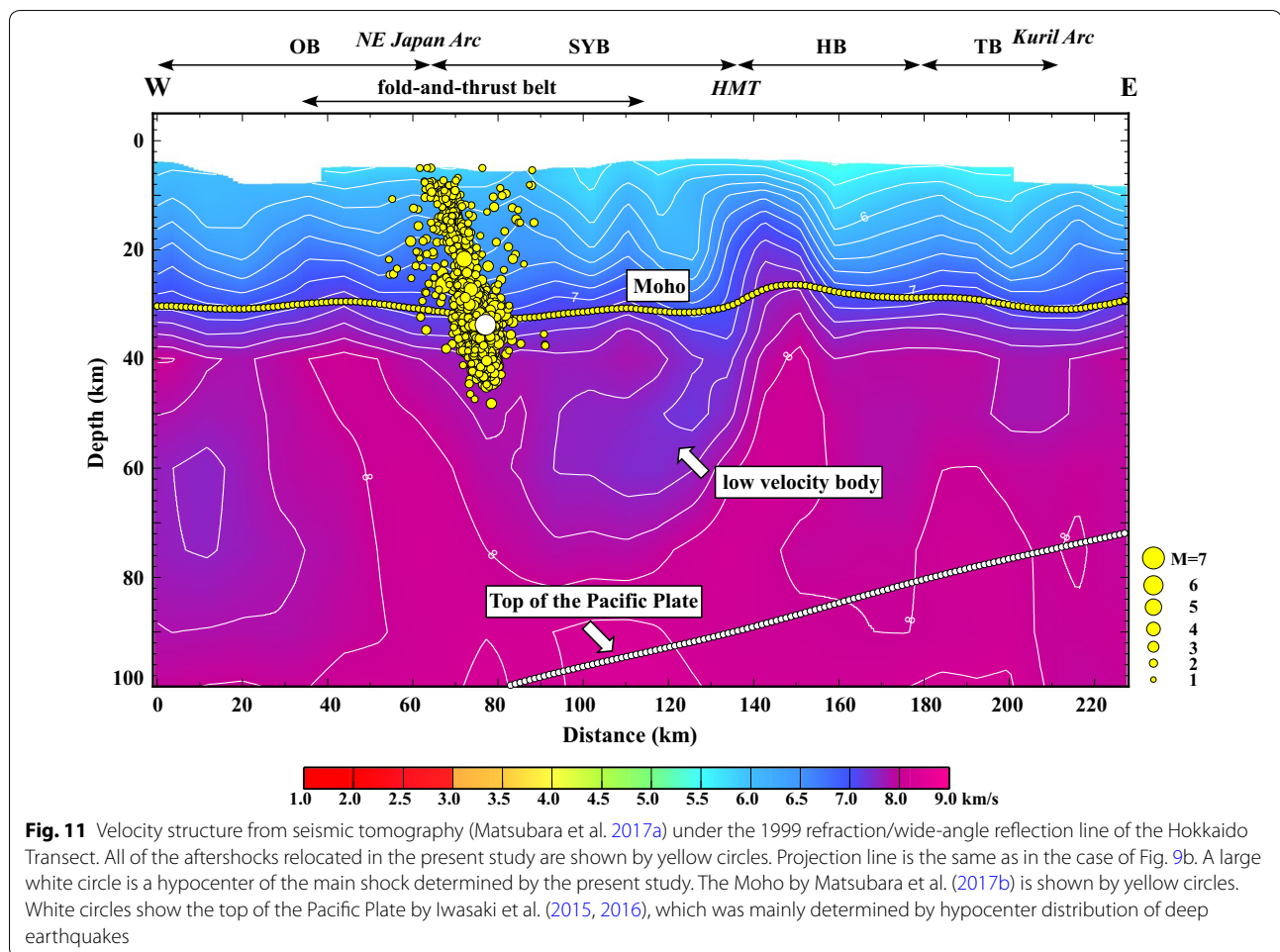
In the following, we discuss several possible explanations for such a deep seismic activity associated with the Iburi Earthquake. First, very low heat flow (< 60 – 80 mW/m²) is observed in the western part of the HCZ including the fold-and-thrust belt (Tanaka et al. 2004). Although the thick sedimentary package (Figs. 3b and 5a) is one of the reasons for such low heat flow (e.g., Morishige 2018), the fact of deep earthquakes occurring at depths greater than 20–30 km indicates that a brittle region extends to a deeper part of the crust or even to the uppermost mantle. As shown in Fig. 1a, the Kuril Trench meets the



Japan Trench off Hokkaido to form complex geometry of the subducted Pacific Plate. This may give serious effect on the thermal structure in the overriding plate. Several authors presented thermal models for such complicated plate subduction, but the low heat flow in the fold-and-thrust belt is still not fully explained (Morishige and van Keken 2014; Wada et al. 2015; Morishige 2018). Morishige (2018) pointed out the importance of the arc-arc collision in understanding the observed heat flow in the western part of the HCZ.

As for the seismic activity in the mantle, we should mention that the mantle beneath the fold-and-thrust belt

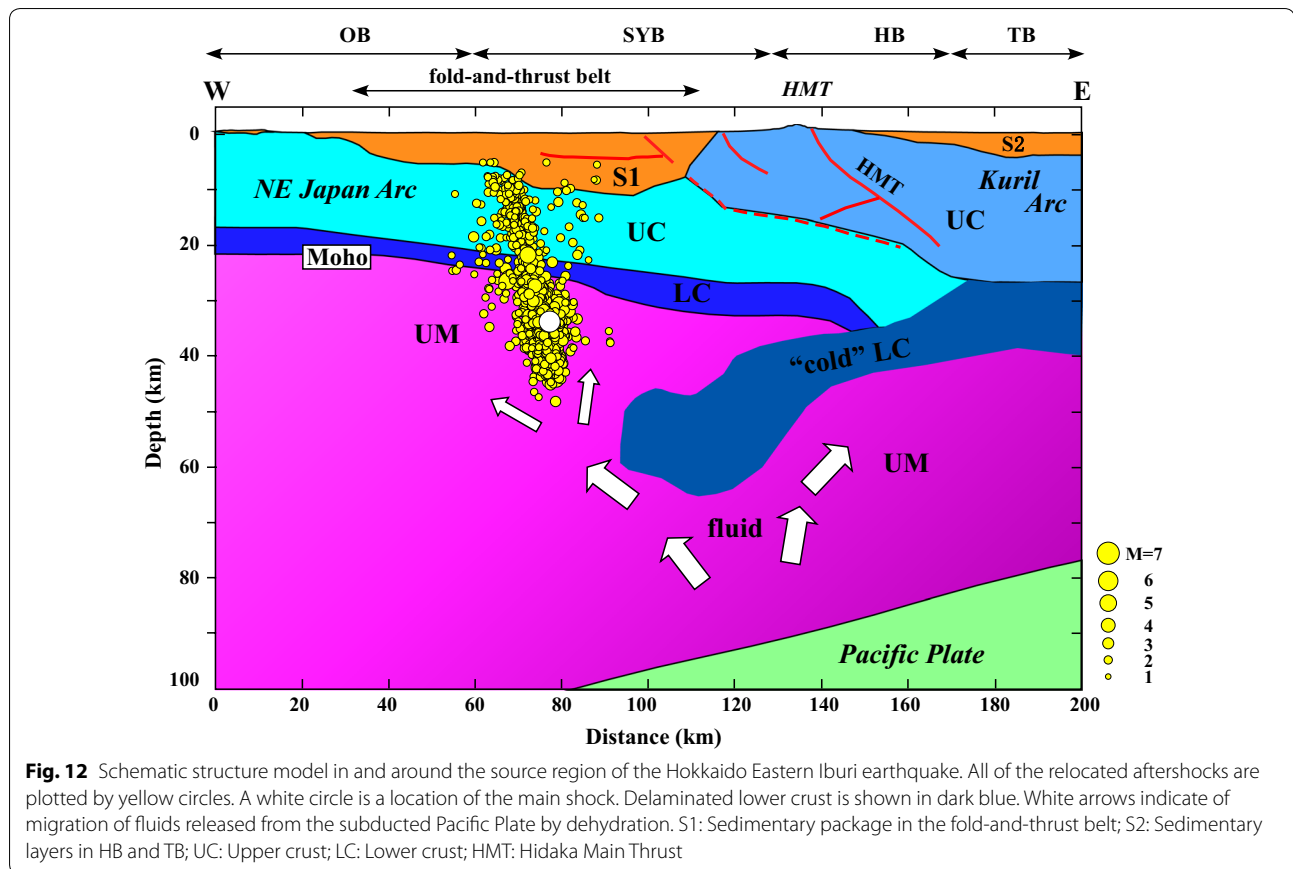
is situated close to the “cold nose” of the forearc region with lower temperature (e.g., Shimamoto 1993; Freed et al. 2016). This low temperature together with the rock composition in the forearc mantle yields a rather high strength and brittle property (Shimamoto 1993). For explaining the seismic activity in the forearc mantle in and off the NE Japan, Uchida et al. (2010) proposed a hypothesis of the detachment and stacking of seamounts from the subducted Pacific Plate by dehydration process. Under the source region of the Iburi Earthquake, however, we have no clear evidence for the existence of subducted seamounts or their fragments. Furthermore,



the plate boundary below the source region is at about 100-km depth (Fig. 11), which is about 40–60-km deeper than in the case of NE Japan. This makes large difference in P–T condition around the plate boundary. So, it is difficult to say that the similar dehydration environment as in the case of the NE Japan is established under our study area.

Another important factor to be taken into account is the arc–arc collision progressing in Central Hokkaido as argued by Morishige (2018). The seismic reflection experiments in 1990s (Arita et al. 1998; Tsumura et al. 1999; Ito 2000, 2002) strongly indicate the crustal delamination in the Kuril Arc side, where the upper 23-km crust is thrust up along the HMT, while the remaining deeper part of the crust descends down to form a wedge-like structure. Such a model of the crustal delamination as mentioned above was supported by Murai et al. (2003), but Kita et al. (2012) proposed a different model where the entire crust and the uppermost mantle in the Kuril Arc side obducts. The tomographic image by Matsubara et al. (2017a), however, shows that

a relatively lower velocity material is descending westward from the Kuril Arc side and situated below the uppermost mantle of the NE Japan side (Fig. 11). The source region of the Iburi Earthquake is located above the western margin of this low velocity body. Figure 12 schematically shows the relationship of the structural heterogeneity around the HCZ and the seismic activity associated with the Iburi Earthquake. If the low velocity body is a lower part of the “cold” crust in the Kuril Arc side, then it directly lowers the forearc mantle temperature (Morishige 2018). Furthermore, such a body becomes an obstacle to the thermal flow within the mantle. Also it prevents the upward migration of fluids released from the subducted plate by dehydration, which suppresses the serpentinization within the forearc mantle. These effects make more preferable environment for brittle fracture in the forearc mantle. Such roles of the deep crustal body were pointed out by Kita et al. (2010) to explain the regional deepening of the upper plane of the double seismic zone beneath the western part of Hokkaido. According to the anisotropic



tomography by Koulakov et al. (2015), the delaminated crust gives significant effects to the mantle flow as well as the movement of fluids supplied from the subducted plate.

The main fracture of the Iburi Earthquake is characterized as a high-angle reverse fault. Such a reverse fault, however, is hardly formed under the present compressional stress regime. Therefore, it is more plausible that this fault structure was originally created by a certain tectonic event before the arc–arc collision started. Based on the compilation of previous geophysical explorations in the southern part of Central Hokkaido, Kuniyasu and Yamada (2004) pointed out the existence of steep faults formed at the times of Late Oligocene to Middle Miocene. The focal mechanism from first motions by JMA (2018c) and NIED (2018) indicates that the rupture of this earthquake was initiated by the strike-slip faulting probably, which seems to occur much easily under the present compressional stress regime, particularly with aid of fluids. Although the system of the fluid supply in the source region of this event is still unknown, it is possible that channels of fluids from the plate by dehydration process are established to generate heterogeneous stress

concentration for brittle fracture around the delaminated lower crust as shown in Fig. 12.

Conclusions

The 2018 Hokkaido Eastern Iburi Earthquake ($M=6.7$) took place under the foreland fold-and-thrust belt of the HCZ at a very deep depth of 37 km with complicated rupture process. To understand the mechanism on the occurrence of such a deep earthquake in relation to the surrounding structural heterogeneity, we reanalyzed controlled source seismic data from the 1998–2000 Hokkaido Transect Project by applying advanced processing techniques including CRS/MDRS stacking method and integrated refraction/wide-angle reflection analyses. The seismic reflection processing imaged for the first time the lower crust and Moho structure of the NE Japan Arc subducted eastward beneath the HCZ. The velocity structure in the fold-and-thrust belt from the refraction/wide-angle reflection data is composed of a very thick (~5–10 km) sedimentary package and the rather thin (16–22 km) NE Japan Arc crust gently descending to the east. The Moho depth under the source area of the Iburi Earthquake is 26–28 km. Based on the structural information mentioned above, the aftershock distribution was

carefully investigated. Relocated aftershocks are distributed in a depth range of 7–45 km showing steep geometry with an eastward dip. We cannot find any evidence on the relationship of the aftershock distribution with the west-verging active fault systems developed in the fold-and-thrust belt. The relocated aftershocks are separated into the upper (7–20 km) and lower (22–45 km) groups. The seismicity gap between them roughly corresponds to the asperity of the Iburi Earthquake (Kobayashi et al. 2019). A large number of events are occurring in the uppermost mantle of the NE Japan Arc. Possible explanation for this deep but high seismic activity is the cold crust delaminated from the Kuril Arc side, which prevents the thermal circulation to cool the forearc mantle and establishes a more favorable environment for brittle failure.

Abbreviations

HB: Hidaka Belt; Hm: Hidaka metamorphic rocks; HMT: Hidaka Main Thrust; Hmz: Hidaka Main zone; Iz: Idon'nappu zone; KGF: Kenomai-Gabari fault; Kz: Kamuikotan zone; Nlz: Nappe of NH; M: Miocene strata; NOF: Nitarachi-Oshorobetsu fault; Pn: Poronai Group; Po: Poroshiri Ophiolite; OB: Oshima Belt; Sr: Sorachi Group; SYB: Sorachi-Yezo Belt; TB: Tokoro Belt; Ynz: Yubetsu-Nakanogawa zone; Yz: Yezo Group.

Acknowledgements

The authors express their sincere thanks to the Research Group for Explosion Seismology, Japan, who acquired refraction/wide-angle reflection data in the 1999 and 2000 experiments of the Hokkaido transect and provided us with opportunities to reanalyze the data. The authors are indebted to Professor Makoto Yamano, Earthquake Research Institute, the University of Tokyo, for providing useful information and suggestions on thermal structure and heat flow in Central Hokkaido. The plate models by Iwasaki et al. (2015) were constructed from topography and bathymetry data by Geospatial Information Authority of Japan (1997), Japan Oceanographic Data Center (2000) and Geographic Information Network of Alaska, University of Alaska (Lindquist et al. 2004). We used Generic Mapping Tools (Wessel and Smith 1998) in most of the figures.

Authors' contributions

Data acquisition in the Hokkaido Transect was done by TIW, TIT, KA, HS, EK, NH, SK and KS together with members of the Research Group for Explosion Seismology, Japan. SA, KN, AF, TIW, NT, SK and TIT performed processing of seismic reflection data. Analysis for the refraction/wide-angle reflection data was done by TIW, NT, EK, NH and KS. MM and NT contributed to the aftershock relocation. Geological interpretation for the obtained results were mainly carried out by TIT, KA, HS, TIW and NT. All of the authors discussed on the contents in this manuscript from various geophysical/geological aspects to polish up them. All authors read and approved the final manuscript.

Funding

The 1999–2000 seismic expeditions were undertaken by the Funds of Special Works of the Earthquake Research Institute, the University of Tokyo, as one of the disciplines of the Japanese New Earthquake Prediction Research Program funded by Ministry of Education, Culture, Sports, Science and Technology, JAPAN (MEXT). The 1998 reflection experiment was supported by MEXT KAK-ENHI (Grand-in-Aid for Scientific Research (A) (2)) 10304033.

Availability of data and materials

The datasets used and/or analyzed during the current study are available from the corresponding author on reasonable request.

Competing interests

The authors declare that they have no competing interests.

Author details

¹ Earthquake Research Institute, the University of Tokyo, Tokyo, Japan. ² Graduate School of Science, Chiba University, Chiba, Japan. ³ Association for the Development of Earthquake Prediction, Tokyo, Japan. ⁴ Hokkaido Research Center of Geology, Sapporo, Japan. ⁵ National Research Institute for Earth Science and Disaster Resilience, Tsukuba, Japan. ⁶ JAPEX, Tokyo, Japan. ⁷ GEOSYS, Inc, Tokyo, Japan. ⁸ Japan Oil, Gas and Metals National Corporation, Tokyo, Japan. ⁹ JGI, Inc, Tokyo, Japan. ¹⁰ Schlumberger Ltd, Doha, Qatar.

Received: 10 March 2019 Accepted: 11 September 2019

Published online: 27 September 2019

References

- Adachi K (2002) The crustal structure beneath the Hidaka Collision Zone, Central Hokkaido, Japan, inferred from seismic refraction/wide-angle reflection and reflection profiling, Master Thesis, Graduate School of Science, the University of Tokyo
- Aoki N, Narahara S, Takahashi A, Nishiki T (2010) Imaging of conflicting dipping events by the multi-dip reflection surfaces method. SEG Expanded Abstract, pp. 3604–3608
- Arita K, Ikawa T, Ito T, Yamamoto A, Saito M, Nishida Y, Satoh H, Kimura G, Watanabe T, Ikawa T, Kutoda T (1998) Crustal structure and tectonics of the Hidaka collision zone, Hokkaido (Japan), revealed by vibroseis seismic reflection and gravity surveys. *Tectonophysics* 290:197–210
- Berkovitch A, Belfer I, Landa E (2008) Multifocusing as a method of improving surface imaging. *Lead Edge* 27:250–256
- Cerveny V (1985) The application of ray tracing to the propagation of shear waves in complex media. In: Dohr G (ed) *Seismic exploration*, vol 15A. Seismic shear waves part a: theory. Geophysical Press, London, pp 1–124
- Finn C (1994) Aeromagnetic evidence for a buried Early Cretaceous magmatic arc, northeast Japan. *J Geophys Res* 99:22165–22185
- Freed AM, Hashima A, Becker TW, Okaya DA, Sato H, Hatanaka Y (2016) Resolving depth-dependent subduction zone viscosity and afterslip from post-seismic displacements following the 2011 Tohoku-oki, Japan earthquake. *Earth Planet Sci Lett* 459:279–290
- Geospatial Information Authority of Japan (1997) Digital map 250 m grid (elevation), Geospatial Information Authority of Japan
- Geospatial Information Authority of Japan (2018) The 2018 Hokkaido Eastern Iburi earthquake: fault model (preliminary) <http://www.gsi.go.jp/cais/topic180912-index-e.html>. Accessed 10 Dec 2018
- Hirata N, Matsu'ura M (1987) Maximum-likelihood estimation of hypocenter with origin time eliminated using nonlinear inversion technique. *Phys Earth Planet Inter* 47:50–61
- Hubral P, Höcht G, Jäger R (1999) Seismic illumination. *Lead Edge* 18:1268–1271
- Ito T (2000) Crustal structure of the Hidaka collision zone and its foreland fold-and-thrust belt, Hokkaido, Japan. *J Jpn Assoc Petrol Technol* 65:103–109 (in Japanese with English abstract)
- Ito T (2002) Active faulting, lower crustal delamination and ongoing Hidaka arc-arc collision, Hokkaido, Japan. In: Fujinawa Y, Yoshida A (eds) *Seismotectonics in convergent plate boundary*. Terrapub, Tokyo, pp 219–224
- Iwasaki T, Hirata N, Suyehiro K, Kanazawa T, Urabe T, Moriya T, Shimamura H (1983) Aftershock distribution of the 1982 Urakawa-Oki earthquake determined by ocean bottom seismographic and land observations. *J Phys Earth* 31:299–328
- Iwasaki T, Ozel O, Moriya T, Sakai S, Suzuki S, Aoki G, Maeda T, Iidaka T (1998) Lateral structural variation across a collision zone in central Hokkaido, Japan, as revealed by wide-angle seismic experiments. *Geophys J Int* 132:435–457
- Iwasaki T, Sato H, Hirata N, Ito T, Moriya T, Kurashimo E, Kawanaka T, Kozawa T, Ichinose Y, Saka M, Takeda T, Kato W, Yoshikawa T, Arita K, Takanami T, Yamamoto A, Toshii T, Ikawa T (2001) Seismic reflection experiment in the northern part of the Hidaka Collision Zone, Hokkaido, Japan. *Bull Earthq Res Inst Univ Tokyo* 76:115–128 (in Japanese with English abstract)
- Iwasaki T, Adachi K, Moriya T, Miyamachi H, Matsushima T, Miyashita K, Takeda T, Taira T, Yamada T, Ohtake T (2004) Upper and middle crustal deformation of an arc-arc collision across Hokkaido, Japan, inferred from seismic refraction/wide-angle reflection experiments. *Tectonophysics* 383:59–73

- Iwasaki T, Sato H, Shinohara M, Ishiyama T, Hashima A (2015) Fundamental structure model of island arcs and subducted plates in and around Japan. Paper presented at 2015 Fall Meeting, American Geophysical Union, San Francisco, Dec. 14–18
- Iwasaki T, Sato H, Shinohara M, Ishiyama T, Hashima A (2016) Plate models in and around Japan (PLMDL_2016), http://evrress.eri.u-tokyo.ac.jp/database/PLATEmodel/PLMDL_2016/. Accessed 15 Dec 2016
- Jäger R, Mann J, Höcht G, Hubral P (2001) Common-reflection-surface stack: image and attributes. *Geophysics* 66:97–109
- Japan Meteorological Agency (2018a) Information on the 2018 Hokkaido Eastern Iburi Earthquake. https://www.jma.go.jp/jma/menu/20180906_iburi_jishin_menu.html. Accessed 20 Dec 2018
- Japan Meteorological Agency (2018b) Centroid Moment Tensor (CMT) solution of an earthquake on Sept. 6, 2018. <https://www.data.jma.go.jp/svd/eqev/data/mech/cmt/fig/cmt20180906030759.html>. Accessed 20 Dec 2018
- Japan Meteorological Agency (2018c) Focal mechanism solutions from first motion data of an earthquake on Sept. 6, 2018. <https://www.data.jma.go.jp/svd/eqev/data/mech/ini/fig/mc20180906030759.html>. Accessed 20 Dec 2018
- Japan Oceanographic Data Center (2000) 500 m gridded bathymetry data. http://www.jodc.go.jp/jodcweb/JDOSS/info/JEGG_j.html. Accessed 25 May 2015
- Kazuka T, Kikuchi S, Ito T (2002) Structure of the foreland fold-and-thrust belt, Hidaka Collision Zone, Hokkaido, Japan: re-processing and re-interpretation of the JNOC seismic reflection profiles 'Hidaka' (H91-2 and H91-3). *Bull Earthq Res Inst Univ Tokyo* 77:97–109 **(in Japanese with English abstract)**
- Kiminami K, Kotani Y (1983) Mesozoic arc-trench systems in Hokkaido, Japan. In: Hashimoto M, Uyeda S (eds) *Accretion tectonics in the circum-Pacific Regions*. Terrapub, Tokyo, pp 107–122
- Kimura G (1986) Oblique subduction and collision: forearc tectonics of the Kuril arc. *Geology* 14:404–407
- Kimura G (1994) The latest Cretaceous-early Paleogene rapid growth of accretionary complex and exhumation of high pressure series metamorphic rocks in northwestern Pacific margin. *J Geophys Res* 99:22147–22164
- Kimura G, Miyashita S, Miyasaka S (1983) Collision tectonics in Hokkaido and Sakhalin in Accretion tectonics. In: Hashimoto M, Uyeda S (eds) *The Circum-Pacific Regions*. Terrapub, Tokyo, pp 123–134
- Kita S, Okada T, Hasegawa A, Nakajima J, Matsuzawa T (2010) Anomalous deepening of a seismic belt in the upper-plane of the double seismic zone in the Pacific slab beneath the Hokkaido corner: possible evidence for thermal shielding caused by subducted crust materials. *Earth Planet Sci Lett* 290:415–426
- Kita S, Hasegawa A, Nakajima J, Okada T, Matsuzawa T, Katsumata K (2012) High-resolution seismic velocity structure beneath the Hokkaido corner, northern Japan: arc-arc collision. *J Geophys Res*. <https://doi.org/10.1029/2012jb009356>
- Kiyokawa S (1992) Geology of the Itonnappu Belt, Central Hokkaido, Japan: evolution of a Cretaceous accretionary complex. *Tectonics* 11:1180–1206
- Kobayashi H, Koketsu K, Miyake H (2019) Rupture process of the 2018 Hokkaido Eastern Iburi earthquake derived from strong motion and geodetic data. *Earth. Planet Sci* 71:63. <https://doi.org/10.1186/s40623-019-1041-7>
- Komatsu M, Miyashita S, Maeda J, Osanai Y, Toyoshima T (1983) Disclosing of a deepest section of continental-type crust up-thrust as the final event of collision of arcs in Hokkaido, North Japan. In: Hashimoto M, Uyeda S (eds) *Accretion tectonics in the Circum-Pacific Regions*. Terrapub, Tokyo, pp 149–165
- Koulakov I, Kukarina E, Fathi IH, Khrepy SE, Al-Arifi N (2015) Anisotropic tomography of Hokkaido reveals delamination-induced flow above a subducting slab. *J Geophys Res* 120:3219–3239. <https://doi.org/10.1002/2014JB011823>
- Kuniyasu M, Yamada Y (2004) Structural styles of deep zones in southern central Hokkaido, northern Japan. *J Jpn Assoc Petrol Technol* 69:131–144 **(in Japanese with English abstract)**
- Lindquist KG, Engle K, Stahlke D, Price E (2004) Global topography and bathymetry grid improves research efforts. *Eos Trans AGU* 85(19):186. <https://doi.org/10.1029/2004EO190003>
- Matsubara M, Sato H, Uehira K, Mochizuki M, Kanazawa T (2017a) Three-dimensional seismic velocity structure beneath Japanese Islands and surroundings based on NIED seismic networks using both inland and offshore events. *J Disaster Res* 12:844–857. <https://doi.org/10.20965/jdr.2017.p0844>
- Matsubara M, Sato H, Ishiyama T, Horne AV (2017b) Configuration of the Moho discontinuity beneath the Japanese Islands derived from three-dimensional seismic tomography. *Tectonophysics* 710–711:97–107
- Miura S, Takahashi T, Nakanishi A, Tsuru T, Kodaira S, Kaneda Y (2005) Structural characteristics off Miyagi forearc region, the Japan Trench seismogenic zone, deduced from a wide-angle reflection and refraction study. *Tectonophysics* 407:165–188
- Miyamachi H, Moriya T (1984) Velocity structure beneath the Hidaka mountains in Hokkaido, Japan. *J Phys Earth* 32:13–42
- Miyamachi H, Kasahara M, Suzuki S, Tanaka K, Hasegawa A (1994) Seismic velocity structure in the crust and upper mantle beneath northern Japan. *J Phys Earth* 42:269–301. <https://doi.org/10.4294/jpe1952.42.269>
- Morishige M (2018) Subduction zone dynamics constrained from numerical models and observations. *Zisin* 71:1–11. <https://doi.org/10.4294/zisin.2017-10> **(in Japanese with English abstract)**
- Morishige M, van Keken PE (2014) Along-arc variation in the 3D thermal structure around the junction between the Japan and Kurile arcs. *Geochem Geophys Geosyst* 15:2225–2240. <https://doi.org/10.1002/2014GC005394>
- Moriya T (1972) Aftershock activity of the Hidaka mountains earthquake of January 21, 1970. *J Seismol Soc Jpn* 24:287–297 **(in Japanese with English abstract)**
- Moriya T, Miyamachi K, Katoh S (1983) Spatial distribution and mechanism solutions for foreshocks, mainshock and aftershocks of the Urakawa-oki Earthquake of March 21, 1982. *Geophys Bull Hokkaido Univ* 42:191–213 **(in Japanese with English abstract)**
- Moriya T, Okada H, Matsushima T, Asano S, Yoshii T, Ikami A (1998) Collision structure in the upper crust beneath the southwestern foot of the Hidaka Mountains, Hokkaido, Japan as derived from explosion seismic observations. *Tectonophysics* 290:181–196. [https://doi.org/10.1016/S0040-1951\(98\)00011-0](https://doi.org/10.1016/S0040-1951(98)00011-0)
- Murai Y et al (2003) Delamination structure imaged in the source area of the 1982 Urakawa-oki earthquake. *Geophys Res Lett* 30(9):1490. <https://doi.org/10.1029/2002GL016459>
- Nakajima J, Matsuzawa T, Hasegawa A (2002) Moho depth variation in the central part of northeastern Japan estimated from reflected and converted waves. *Phys Earth Planet Inter* 130:31–47
- Nanayama F, Kanamatsu T, Fujiwara Y (1993) Sedimentary petrology and paleotectonic analysis of the arc-arc junction: the Paleocene Nakanogawa Group in the Hikaka Belt, central Hokkaido, Japan. *Palaeogeogr Palaeoclim Palaeoecol* 105:53–69
- National Research Institute for Earth Science and Disaster Resilience (2018) Back number of recent large earthquakes (in Japanese). <http://www.hinet.bosai.go.jp/backnumber/?LANG=en&y=2018&m=09>. Accessed 20 Dec. 2018
- Niida K, Kito N (1986) Cretaceous arc-trench systems in Hokkaido. *Monogr. Assoc. Geol. Collab. Jpn.* 31:379–402 **(in Japanese with English abstract)**
- Omuralieva AM, Hasegawa A, Matsuzawa T, Nakajima J, Okada T (2012) Lateral variation of the cutoff depth of shallow earthquakes beneath the Japanese Islands and its implications for seismogenesis. *Tectonophysics* 518–521:93–105. <https://doi.org/10.1016/j.tecto.2011.11.013>
- Shimamoto T (1993) Rheology of rocks and plate tectonics. In: Hudson JA, Brown ET (eds) *Comprehensive rock engineering*, vol 1. Pergamon Press, Oxford, New York, pp 93–109
- Takahashi N, Kodaira S, Tsuru T, Park J-O, Kaneda Y, Suyehiro K, Kinoshita H, Abe S, Nishino M, Hino R (2004) Seismic structure and seismogenesis off Sanriku region, northeastern Japan. *Geophys J Int* 159:129–145. <https://doi.org/10.1111/j.1365-246X.2004.02350.x>
- Takanami T (1982) Three-dimensional seismic structure of the crust and upper mantle beneath the orogenic belts in southern Hokkaido, Japan. *Phys Earth* 30:87–104. <https://doi.org/10.4294/jpe1952.30.87>
- Tanaka A, Yamano M, Sasada M (2004) Geothermal gradient and head flow data in and around Japan. Digital Geoscience Map DGM P-5, Geological Survey of Japan
- The Headquarters for Earthquake Research Promotion (2018a) Evaluation of the Hokkaido Eastern Iburi earthquake (September 6, 2018). <https://www.jishin.go.jp/main/index-e.html>. Accessed 10 Dec 2018

- The Headquarters for Earthquake Research Promotion (2018b) Evaluation of the Hokkaido Eastern Iburu Earthquake (September 11, 2018). <https://www.jishin.go.jp/main/index-e.html>. Accessed 10 Dec 2018
- The Headquarters for Earthquake Research Promotion (2018c) Evaluation of the Hokkaido Eastern Iburu Earthquake (October 12, 2018). <https://www.jishin.go.jp/main/index-e.html>. Accessed 10 Dec 2018
- The Research Group for Explosion Seismology, Japan (2002a) Seismic refraction/wide-angle reflection experiment across the Hidaka collision zone, Hokkaido (Ohtaki-Urahoro profile). *Bull Earthq Res Inst Univ Tokyo* 77:139–172 **(in Japanese with English abstract)**
- The Research Group for Explosion Seismology, Japan (2002b) Seismic refraction/wide-angle reflection experiment across the foreland area of the Hidaka collision zone, Hokkaido (Ohtaki-Biratori profile). *Bull Earthq Res Inst Univ Tokyo* 77:173–198 **(in Japanese with English abstract)**
- Tsumura N, Ikawa H, Ikawa T, Shinohara M, Ito T, Arita K, Moriya T, Kimura G, Ikawa T (1999) Delamination-wedge structure beneath the Hidaka Collision Zone, Central Hokkaido, Japan inferred from seismic reflection profiling. *Geophys Res Lett* 26:1057–1060
- Uchida N, Kriby SH, Okada T, Hino R, Hasegawa A (2010) Supraslab earthquake clusters above the subduction plate boundary offshore Sanriku, north-eastern Japan: seismogenesis in a graveyard of detached seamounts? *J Geophys Res* 115:B09308. <https://doi.org/10.1029/2009JB006797>
- Ueda H (2005) Accretion and exhumation structures formed by deeply subducted seamounts in Kamuikotan high-P/T Zone, Hokkaido. *Tectonics* 24(TC2007):1–17
- Ueda H (2016) Hokkaido. In: Moreno T, Wallis S, Kojima T, Gibbons W (eds) *The geology of Japan*. Geological Society, London, pp 201–221
- Ueda H, Kawamura M, Iwata K (2001) Tectonic evolution of Cretaceous accretionary complex in the Ido-nappu Zone, Urakawa area, central Hokkaido, Northern Japan: with reference to radiolarian ages and thermal structure. *J Geol Soc Jpn* 107:81–98
- Wada I, He J, Hasegawa A, Nakajima J (2015) Mantle wedge flow pattern and thermal structure in Northeast Japan: effects of oblique subduction and 3-D slab geometry. *Earth Planet Sci Lett* 426:76–88
- Wessel P, Smith WHF (1998) New improved version of the generic mapping tools released. *Eos Trans AGU* 79:579
- Yamamoto Y, Obana K, Kodaira S, Hino R, Shinohara M (2014) Structural heterogeneities around the megathrust zone of the 2011 Tohoku earthquake from tomographic inversion of onshore and offshore seismic observations. *J Geophys Res Solid Earth* 119:1165–1180. <https://doi.org/10.1002/2013JB010582>
- Zelt CA, Barton PJ (1998) Three-dimensional seismic refraction tomography: a comparison of two methods applied to data from the Faeroe Basin. *J Geophys Res* 103:7187–7210

Publisher's Note

Springer Nature remains neutral with regard to jurisdictional claims in published maps and institutional affiliations.

Submit your manuscript to a SpringerOpen® journal and benefit from:

- Convenient online submission
- Rigorous peer review
- Open access: articles freely available online
- High visibility within the field
- Retaining the copyright to your article

Submit your next manuscript at ► [springeropen.com](https://www.springeropen.com)
